Catalysis Today 152 (2010) 48–53

Contents lists available at ScienceDirect

Catalysis Today

journal homepage: www.elsevier.com/locate/cattod

Acidic and catalytic properties of silica modified by iron oxide nanoparticles

Tatiana Rostovshchikova [a,*], Vladimir Smirnov [a], Olga Kiseleva [a], Valentina Yushcenko [a], Mark Tzodikov [b], Yurii Maksimov [c], Igor Suzdalev [c], Leonid Kustov [d], Olga Tkachenko [d]

[a] Lomonosov Moscow State University, Leninskie Gory, Moscow, 119991, Russia
[b] Topchiev Institute of Petrochemical Synthesis, RAS, Leninskii prospect, 29, Moscow, 119991, Russia
[c] Semenov Institute of Chemical Physics, RAS, Kosygina street, 4, Moscow, 119991, Russia
[d] Zeliskii Institute of Organic Chemistry, RAS, Leninskii prospect, 47, 119991, Moscow, Russia

ARTICLE INFO

Article history:
Available online 5 December 2009

Keywords:
Silica
Iron oxide
Structure
Size
Acidity
Catalysis
Alkylation

ABSTRACT

Relations between the catalyst structure, acid and catalytic properties of two types of silica (silica gel and layer silica) modified by γ-ferric oxide nanoparticles of a different size (2–4 and 8–10 nm) were studied in the benzene alkylation by benzyl chloride. The catalysts were characterized by means of Mossbauer spectroscopy, temperature programmed NH_3 desorption and diffuse reflectance infrared Fourier transform spectroscopy (DRIFT) using CO and CD_3CN as test molecules. It was found that the particle size and the silica structure strongly affect the catalytic behavior.

1. Introduction

Iron-containing heterogeneous catalysts are interesting for Friedel–Crafts alkylation due to their redox function and acid properties [1–3]. It was surprising that Fe^{3+}-containing catalysts are more active in these reactions compared to Al^{3+}-containing catalysts. Strong acidic catalysts, except sulfated Fe_2O_3, show only poor activity for the benzylation of benzene [1]. It has been found previously [4] that iron oxide nanoparticles supported on silica are more efficient and selective for benzene alkylation by allyl chloride and dichlorobutene isomerization, than corresponding bulk oxides. Bulk iron oxide causes mostly oligomerization of chloroolefins while no products of oligomerization were detected when iron oxide nanoparticles were used. The following factors strongly affect the catalytic behavior of iron oxide nanoclusters: the nature of iron precursors, the structure of silica support, the routine of pretreatment of support and the total iron oxide content [5,6]. These factors control the catalyst composition, nanocluster size and structure as well as the catalytic activity. The catalytic activity in the chloroolefin reactions studied increases in order of iron oxides α-$Fe_2O_3 < Fe_3O_4 < \gamma$-$Fe_2O_3$. The spinel structure of γ-Fe_2O_3 is favorable for catalysis as it has been observed for alkylation and oxidation reactions [3,7–9]. Analysis of the Mossbauer spectra and magnetic properties of catalysts together with catalytic studies allowed us to suggest that the interaction of the γ-Fe_2O_3 nanoclusters with chloroolefin resulted in the reduction of Fe^{3+} ions to Fe^{2+} ions that were bound in the catalytic active mixed-valence complex containing Cl^- and O^{2-} ions as ligands [4]. The extensive reduction and chlorination of Fe_2O_3 resulting in the $FeCl_2 \cdot nH_2O$ formation is a reason of the catalyst deactivation. Catalysts prepared on layer silica are more active and stable in the chloroolefin reactions compared to that prepared on silica gel [5,6].

The purpose of this work is to elucidate the role of particle size and silica structure on the acidic and catalytic properties of γ-Fe_2O_3 nanoparticles supported on two types of silica: the activated silica gel matrix (AMG) prepared from silica gel and the activated silica matrix (AMS) prepared from the natural mineral vermiculite of layer structure [9] by means of acidic treatment. The activities of catalysts with different iron content between 2.5 and 18 wt.% were tested in the benzene alkylation by benzyl chloride resulting in the diphenylmethane formation. The results were compared with data obtained previously for the benzene alkylation by allyl chloride [4,6].

2. Experimental

2.1. Catalyst preparation

The activated matrix of silica gel (AMG) was prepared from mesoporous silica gel (MSG, 340 m^2/g) by the two stage acidic etching with 5–7% and 36% hydrochloric acid followed by calcination at 400 °C.

* Corresponding author. Tel.: +7 4959393498; fax: +7 4959328846.
E-mail address: rtn@kinet.chem.msu.ru (T. Rostovshchikova).

0920-5861/$ – see front matter © 2009 Elsevier B.V. All rights reserved.
doi:10.1016/j.cattod.2009.10.017

Table 1
Mossbauer parameters of the Fe sites in AMG and AMS catalysts with different iron content (δ is isomer shift, relative to α-Fe; Δ is quadruple shift or quadruple splitting; Γ is line width, H_{in} is internal magnetic field).

Catalyst	Fe (%)	Component	δ	Δ ±0.03 мм/с	Γ	H_{in} ±0.5 T	Relative content (%) ±0.5%
Fe/AMG	2.5	Fe^{3+}-paramagnetic	0.34	0.93	0.62	–	100
		Fe^{3+}-paramagnetic	0.34	0.87	0.58	–	89
	5.0	$Fe_3O_{4+\delta}$ (A)[a]	0.30	−0.06	0.65	46.8	6
		$Fe_3O_{4+\delta}$ (B)[a]	0.70	0.00	1.10	44.7	5
		Fe^{3+}-paramagnetic	0.35	0.85	0.54	–	74
	18	$Fe_3O_{4+\delta}$ (A)[a]	0.34	0.04	0.70	47.0	10
		$Fe_3O_{4+\delta}$ (B)[a]	0.68	-0.08	1.30	43.7	16
Fe/AMS[b]	2.5	Fe^{3+}-paramagnetic	0.33	0.97	0.58	–	100
	4.5	Fe^{3+}-paramagnetic	0.33	1.05	0.58	–	66
		γ-Fe_2O_3	0.33	−0.06	0.71	49.6	34
	18	Fe^{3+}-paramagnetic	0.34	1.05	0.61	–	50
		γ-Fe_2O_3	0.34	0.02	0.66	49.4	50

[a] A and B, tetrahedral and octahedral sites occupied by Fe ions in the structure of non-stoichiometric magnetite.
[b] Data [6].

The activated matrix of layer silica (AMS, 350 m^2/g) was produced from the natural mineral "vermiculite" [9] by selective acidic etching with 5–7% hydrochloric acid and a mixture of 40% sulfuric and 60% nitric acids followed by calcination at 400 °C.

The catalysts with Fe content ranging 2.5–18 wt.% were prepared by the impregnation of a support with an excess of a solution of $Fe(acac)_3$ in toluene with calculated Fe content. After the discoloration (5–6 h) an excess of the solution was removed. The catalyst were dried in air at 400 °C (2 h). Before catalytic experiments catalysts were activated at 100 °C in air.

2.2. Catalyst characterization

All catalysts on AMG were X-ray amorphous, they were studied in detail by means of Mossbauer spectroscopy as it was described [4].

Textural properties (BET surface area, average pore volume and size) of samples were measured by N_2 physisorption at −196 °C usingASAP-2000 Micromeritics setup. Before the N_2 adsorption samples were heated for 2 h at 300 °C in a vacuum. Isotherms were registered as dependencies V_{ads} (cm^3/g) = $f(p/p_0)$. A surface area was calculated via BET method basing on received N_2 adsorption isotherms; a pore volume distribution was calculated by BGH method; calculations were performed using Micrometrics software pack.

The examination of acid sites of catalysts was performed by means of the temperature programmed desorption (TPD) of NH_3 and the diffuse reflectance IR-spectroscopy using CO and CD_3CN as test molecules. Prior to TPD the samples were heated at 50 °C for 4 h, blown with NH_3, and cooled to room temperature in He atmosphere.

Diffuse reflectance infrared Fourier transform (DRIFT) spectra were recorded at room temperature with a Nicolet 460 Protégé spectrometer equipped with a diffuse reflectance attachment. The catalyst sample was placed in an ampoule supplied with a KBr window and pretreated in situ for 2 h at 350 °C in a vacuum to remove physical adsorbed water. All spectra were collected with 200 scans in the range of a 400–6000 cm^{-1} with a resolution of a 4 cm^{-1}. The probe molecules were adsorbed at room temperature and the equilibrium pressure of 10 Torr (CO) and at the saturated vapor pressure 96 Torr (CD_3CN).

2.3. Catalytic experiments

The benzene alkylation by benzyl chloride was carried out at 60–90 °C in the stirred glass ampoules as it was described for chloroolefin reactions [4]. The reaction mixture (0.2 ml) contained benzene and benzyl chloride (4:1). The amount of a catalyst was varied between 0.001 and 0.01 g depending on Fe content. The Fe content in reaction mixture was the same in all experiments. The products were analyzed by means of gas chromatography. Diphenylmethane was the only reaction product. The values of overall catalytic activity were expressed by mole of product per mole of iron in hour for the highest reaction rate. In contrast to the chloroolefin reactions [4], the rate of benzylation was not sensitive to the presence of oxygen.

3. Results and discussion

3.1. Catalyst characterization

Some catalyst characteristics were described in previous papers [4–6]. Mossbauer parameters of the iron sites in γ-Fe_2O_3 catalysts on AMS and AMG are summarized in Table 1. Mossbauer spectra and magnetic properties of samples with low (2.5 wt.%) Fe content on both types of silica prepared using $Fe(acac)_3$ as a precursor were similar [6]. These catalysts contained only small superparamagnetic γ-Fe_2O_3 clusters with the size not above 2–4 nm. It was found that the samples with 4.5% and 18%Fe prepared on AMS, in addition to small superparamagnetic γ-Fe_2O_3 clusters, contained also large magnetically ordered γ-Fe_2O_3 clusters with the size d ~8–10 nm [6]. For the 4.5%Fe/AMS and 18%Fe/AMS catalysts the intensity ratio of HFS lines related to magnetically ordered clusters increased from ~0.37 to ~0.5. The different picture was observed when catalysts were prepared on AMG support. Mossbauer spectra of these catalysts with Fe content between 2.5% and 18% are shown in Fig. 1. One can see that the doublet describing "paramagnetic" high-spin Fe^{3+} sites in the octahedral surrounding of O^{2-} ions dominates in all spectra. In accordance with parameters of Mossbauer spectra given in Table 1, the catalysts with the high Fe content on AMG contain also the non-stoichiometric magnetite, in addition to the prevailing superparamagnetic γ-Fe_2O_3 clusters [10]. The partial reduction of iron (III) oxide proceeds during the catalyst preparation using $Fe(acac)_3$ as a precursor due to reductive ability of acetyl acetone and its compounds. This reduction becomes possible only when the high concentration of $Fe(acac)_3$ was used to prepare catalyst with 4.5% and 18%Fe content and when silica gel was used as a support. It is interesting to note that small γ-Fe_2O_3 clusters on AMG are not reduced by H_2 in the temperature below 700 °C. Distinctions in the catalyst structure prepared on silica supports of two types are associated with the different strength of an oxide–oxide interaction between supported iron oxide and silica. The slight interaction of iron oxide and AMG results in only small clusters formation and their partial reduction during the synthesis. By contrast, the presence of strong

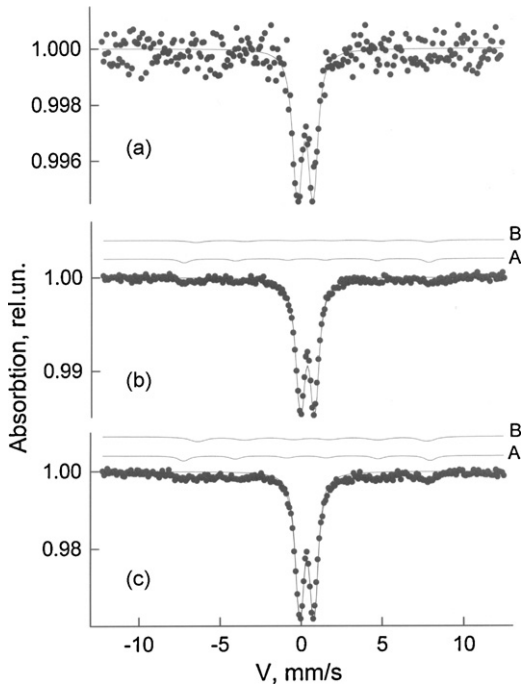

Fig. 1. Mossbauer spectra (room temperature) of AMG catalysts with different Fe content: (a) 2.5%; (b) 5%; (c) 18%.

adsorption sites on the surface of layered silica [9] results in large cluster formation, and the strong interaction between iron oxide and AMS inhibits the iron (III) oxide reduction. Only γ-Fe_2O_3 particles were formed in this case.

The textural properties of catalysts given in Table 2 provided support for these results. Actually the BET surface area does not change when small clusters are supported on AMG, and strongly reduces when large particles are supported on AMS. One can see from these data that the pore diameter does not affect the particle size. Catalysts on AMG with the large pore size contain mostly small clusters. The specific features of layer silica associated with the strong affinity to iron ions [9] and its ability to swell in organic reagents [11] provide a possibility for the formation of large iron oxide particles. The increase of the total pore or adsorption volume for the sample 18% Fe/AMS in two times in comparison with AMS support (Table 2) may be related to AMS swelling during the catalyst preparation.

The results of NH_3 TPD studies of two types of silica before and after their modification by γ-Fe_2O_3 nanoparticles are summarized in Fig. 2 and in Table 2. One can see from these data that a number of acid sites decreased in all cases when small (2–4 nm) iron oxide particles are dominant in the catalyst. Only for the 18%Fe/AMS catalyst containing large (8–10 nm) particles a number of acid sites slightly increased. In accordance with the low temperatures of NH_3 desorption one can conclude that all catalysts contain only slight acid sites closely related to weak Broensted acid sites on the surface of silica supports in the strength of acidity. Only for the 18%Fe/AMG catalyst the peak desorption temperature is shifted to 145 °C. These catalysts containing non-stoichiometric magnetite,

Table 2
Physico-chemical characteristics of catalysts and supports.

Silica		SG	AMG	AMS	AMG			AMS		
Fe (%)		–	–	–	2.5	5.0	18.0	2.5	4.5	18.0
Catalyst composition	Particle size, nm					2–3		2–3	2–3 8–10	2–3 8–10
	The main phase					γ-Fe_2O_3			γ-Fe_2O_3	
	Additional phase					$Fe_3O_{4+\delta}$	$Fe_3O_{4+\delta}$			
Textural properties	S (m^2/g)	340	145	350			140			210
	V_p (cm^3/g)	1.0–1.2	0.9	0.1–0.2			0.8			0.3
	d_p (nm)	12–15	21	7–8			19			5
Acidic properties (NH_3 TPD)	A_n (μmol/g)		297	410	106	103	121	317		446
	T_{max} (°C)		123	124	135	136	145	114		118
	E_{des} (kJ/mol)		99	90	103	105	108	96		97

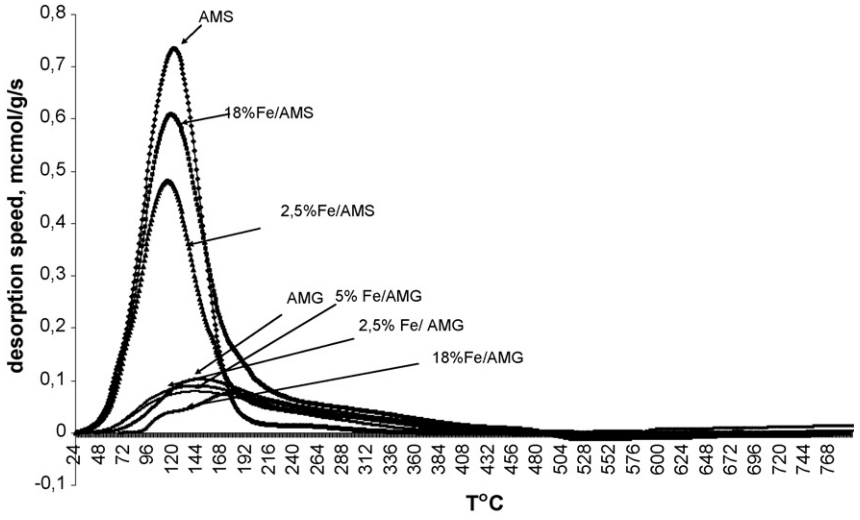

Fig. 2. NH_3 temperature programmed desorption of AMG and AMS parent supports and catalysts with different Fe content.

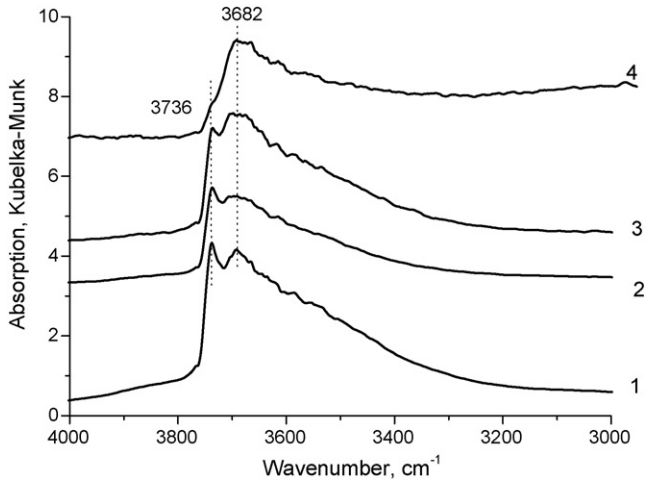

Fig. 3. DRIFT spectra in the OH vibration range: (1) AMS parent support; (2) 2.5%Fe/AMS; (3) 4.5%Fe/AMS; (4) 18%Fe/AMS.

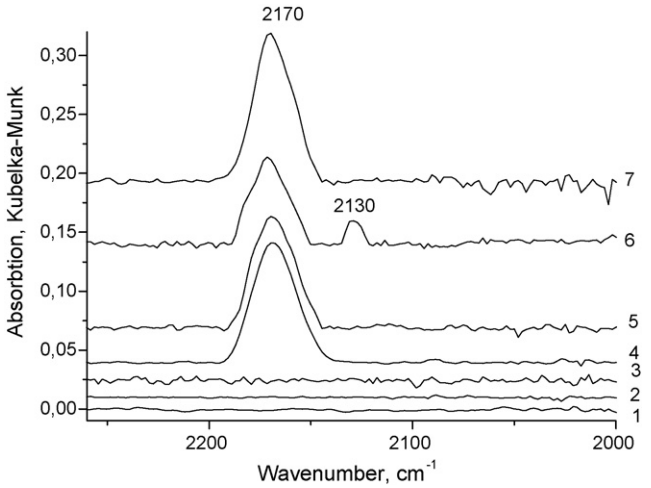

Fig. 5. DRIFT spectra of CO adsorbed on: AMS (1); AMG (2); 18%Fe/AMS (3); 2.5%Fe/AMS (4); 4.5%Fe/AMS (5); 18%Fe/AMG (6) and 2.5%Fe/AMG (7).

in addition to small γ-Fe_2O_3, slightly surpass the catalysts with only γ-Fe_2O_3 nanoparticles in the strength of acidity. To distinguish a nature of acid sites of catalysts DRIFT spectroscopic studies were performed.

3.2. DRIFT spectroscopic studies

The DRIFT spectra of parent AMS and AMG supports and Fe-containing samples in the OH stretching vibration region are shown in Figs. 3 and 4. The band at 3736 cm^{-1} belongs to isolated or terminal hydroxyl groups (weak Broensted acid sites). The band at 3682 cm^{-1} belongs probably to vicinal (involved in hydrogen bonding) OH-groups (moderate Broensted acid sites) [12]. The impregnation of parent supports by $Fe(acac)_3$ results in the decrease of the amount of free silanol groups. This result is in a good agreement with the data obtained by NH_3 adsorption.

Fig. 5 shows the DRIFT spectra collected in the presence of CO. The band of CO stretching vibration at 2170 cm^{-1} is observed in the spectrum of 2.5%Fe/AMG, 18%Fe/AMG, 2.5%Fe/AMS and 4.5%Fe/AMS samples. An additional CO band at 2130 cm^{-1} is observed in the spectrum of 18%Fe/AMG sample, whereas no CO bands are observed in the spectra of 18%Fe/AMS sample and parent AMS and AMG supports. The band at 2170 cm^{-1} is characteristic of the linear adsorbed CO on Fe^{3+} cations and/or Fe(III) oxide [13]. The band at 2130 cm^{-1} belongs to the linear adsorbed CO on Fe^{2+} cations and/or Fe(II) oxide Fe_3O_4 [12–14]. The lack of CO band in the spectrum of 18%Fe/AMS sample can be explained by a small amount of adsorbed CO molecules as a consequence of the low dispersion of iron oxide on the surface of this sample or/and of the blocking of the cavities between the silica layers by large iron oxide particles. The presence of large iron oxide particles (8–10 nm) along with small ones (2–4 nm) was found by volume sensitive method of Mossbauer spectroscopy in 18%Fe/AMS sample as well.

Fig. 6 shows the DRIFT spectra collected in the presence of CD_3CN. The bands of C≡N stretching vibration at 2273 cm^{-1}, which are characteristic of CD_3CN adsorption on Broensted acid sites involved in low hydrogen bonding [15–17], are observed in all spectra. These proton sites possess comparatively low acidity, the blue shift of C≡N stretching vibration as the result of CD_3CN adsorption on these sites is 20 cm^{-1} as compared with the frequency in the gas phase (2253 cm^{-1}) [18]. Moreover the comparison of Fe-containing samples shows (Fig. 7) that the energy of hydrogen bond of CD_3CN molecules with surface OH-groups is higher in sample supported on AMS as compared with

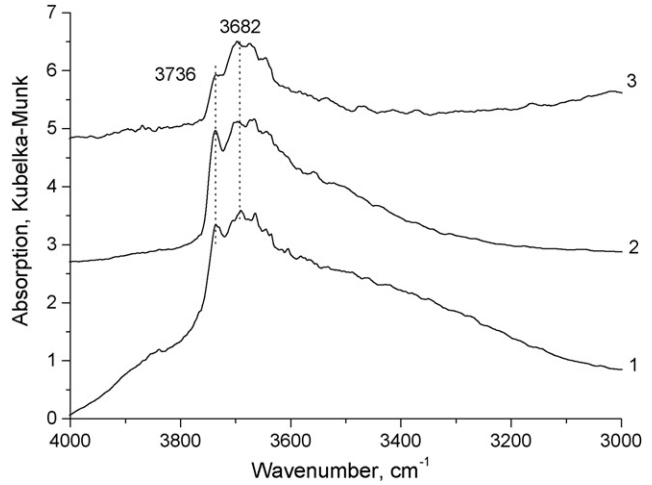

Fig. 4. DRIFT spectra in the OH vibration range: (1) AMG parent support; (2) 2.5%Fe/AMG; (3) 18%Fe/AMG.

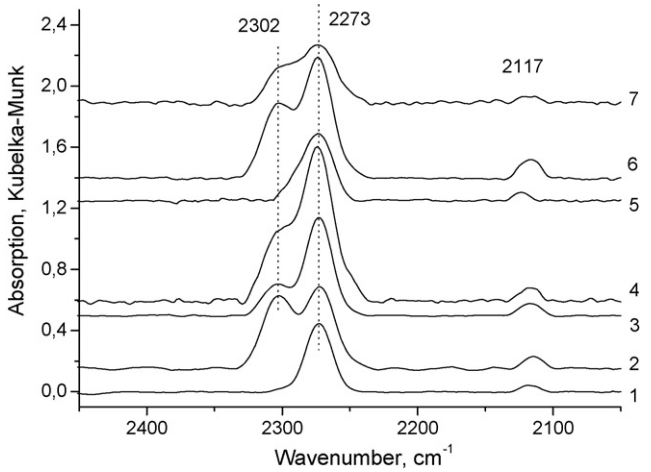

Fig. 6. DRIFT spectra of CD_3CN adsorbed on: AMS (1); 2.5%Fe/AMS (2); 4.5%Fe/AMS (3); 18%Fe/AMS (4); AMG (5); 2.5%Fe/AMG (6) and 18%Fe/AMG (7).

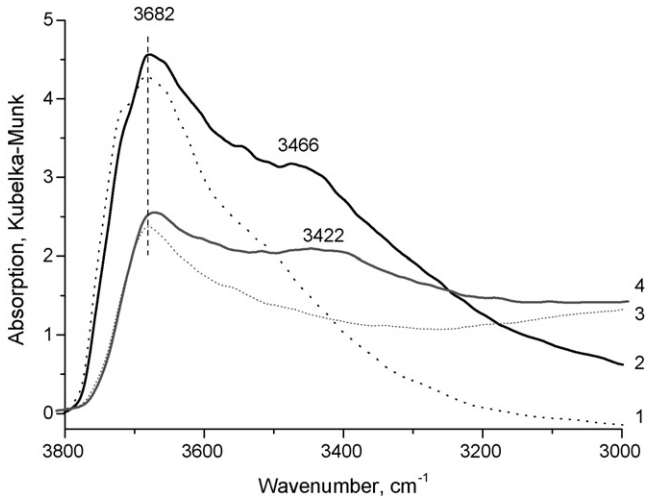

Fig. 7. DRIFT spectra in the OH vibration range before (dot) and after (solid) CD_3CN adsorption: (1 and 2) 2.5%Fe/AMG; (3 and 4) 18%Fe/AMS.

Table 3
Conversion of benzyl chloride (BC) in the benzene benzylation at 60 °C.

Silica	Fe (%)	BC Conversion (%) in time (min)		
		40	60	75
Silica gel	2.5	–	12	21
AMG	2.5	3	45	54
	5.0	5	93	95
	18.0	35	100	100
AMS	2.5	–	1	5
	4.5	1	15	27
	18	3	67	92

sample supported on AMG [19]. The red shift of O-H stretching vibration is 260 cm^{-1} for 18%Fe/AMS and only 216 cm^{-1} for 2.5%Fe/AMG. Therefore the samples supported on AMS possess higher Broensted acidity or proton-donor ability.

Besides the band of C≡N stretching vibration at 2302 cm^{-1} is observed in the spectra of Fe-containing samples (Fig. 6). This band is characteristic of the CD_3CN adsorption on Lewis acid sites (or cationic species). The blue shift of C≡N stretching vibration as the result of CD_3CN adsorption on these acid sites is 49 cm^{-1} as compared with the frequency in the gas phase. Moreover the band of C–D deformation vibration at 2117 cm^{-1} is observed in all spectra. The strength of Lewis acidity in all Fe-containing samples is about the same.

3.3. Catalysis

The benzylation of benzene resulting in only diphenylmethane formation proceeds quantitatively in the presence of modified AMG and AMS at temperature 70–90 °C. The catalysts, prepared using silica gel without the acidic pretreatment, were less active. For example, the conversion of benzyl chloride in 30 min is only 8% at 90 °C for catalyst with 2.5% Fe on silica gel and it achieves 93% at 70 °C for 2.5% Fe/AMG. To elucidate the features of catalytic behavior of modified AMG and AMS associated with the catalyst structure the reaction was carried out at 60 °C. At this temperature the diphenylmethane formation proceeds after the 15 and 60 min induction period for catalysts on AMG and AMS. The results are summarized in Table 3. Catalytic activities of different catalysts in benzylation at 70 °C are shown in Fig. 8 in comparison with data for benzene alkylation by allyl chloride studied previously [4]. One can see from these data the difference in the catalytic behavior of catalysts prepared on AMG and AMS in two processes of alkylation. For benzyl chloride, AMG catalysts are more active compared to AMS catalysts. For allyl chloride, the catalytic activities on both supports are similar with one exception of more active 4.5%Fe/AMS catalyst.

The catalytic activity in the benzylation increases with the growth of Fe content for both types of catalysts. It may be accounted for by the slight growth of the acid strength for the AMG catalyst containing additionally the non-stoichiometric magnetite and by higher Broensted acidity or proton-donor ability of AMS catalyst with 18% Fe content. The catalytic activity in benzylation becomes ten times higher when catalysts were activated at 100 °C and it only reduces when the activation temperature was 400 °C. The reduction of the Broensted acidity may be a reason behind the catalyst deactivation after calcinations at high temperatures [3]. The difference in catalytic activity of catalysts on AGM and AMS may be also associated with the cluster location on the surface of silica or in the space of interplane cavity of layer silica and their availability for reagents [4]. The increase of catalytic activity with the growth both of iron loading and particle size for AMS can be caused by the removal of diffusion limitations that are related to the layered structure of silica [11]. With the growth of particle size up to 8–10 nm in 4.5% and 18%Fe/AMS catalysts a major part of cluster is arranged on a surface of the layer silica close to the mouth of the cavities and becomes accessible to organic molecules [4].

In contrast to the benzylation of benzene, the benzene alkylation by allyl chloride is less sensitive to the catalyst structure and acidity as well as the activation temperature. This fact may be associated with the ability of chloroolefins to reduce iron oxide nanoparticles [4]. The self-organization of the high active catalytic center containing Fe^{3+} and Fe^{2+} ions and Cl^- and O^{2-} ions as ligands becomes possible in the reactions of chloroolefins [6].

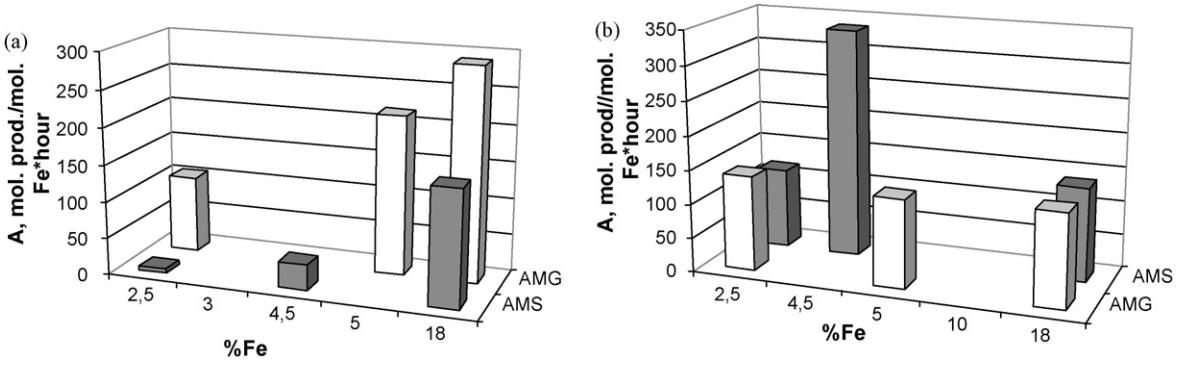

Fig. 8. Catalytic activity of different catalysts in the benzene alkylation by benzyl chloride at 70 °C (a) and by allyl chloride at 110 °C (b).

4. Conclusions

Both acidic and catalytic properties are the function of iron oxide particle size and silica structure. Catalysts prepared on the activated silica gel, and containing non-stoichiometric magnetite, in addition to small γ-Fe_2O_3 particles, are more active in the benzene alkylation by benzyl chloride compared to that prepared on the layer silica. The activity of catalysts on the layered silica increases with the growth both of iron loading and particle size. The different availability of small and large iron oxide clusters deposited on silica gel and layer silica together with the different acidic properties of silica modified of iron oxide nanoparticles are responsible for their catalytic behavior in the benzylation of benzene.

Acknowledgement

The work was supported by RFBR (08-03-92502-NTsNIL-a).

References

[1] V.R. Choudrary, S.K. Jana, Appl. Catal. A: Gen. 224 (2002) 51.
[2] M. Salavati-Nissari, J. Hasanalian, H. Najafian, J. Molec, Catal. A: Chem. 209 (2004) 209.
[3] N.B. Shrigadi, A.B. Shinde, S.D. Samant, Appl. Catal. A: Gen. 252 (2003) 23.
[4] M.V. Tsodikov, T.N. Rostovshchikova, V.V. Smirnov, O.I. Kiseleva, Yu.V. Maksimov, I.P. Suzdalev, V.N. Ikorskii, Catal. Today 105 (2005) 634.
[5] T.N. Rostovshchikova, M.V. Tzodikov, O.V. Buchtenko, V.V. Smirnov, O.I. Kiseleva, Yu.V. Maksimov, D.A. Pankratov, Russ. Chem. Bull. Int. Ed. 54 (2005) 1418.
[6] T.N. Rostovshchikova, O.I. Kiseleva, V.V. Smirnov, Yu.V. Maksimov, I.P. Suzdalev, V.E. Prusakov, M.V. Tsodikov, V.N. Ikorskii, Russ. Chem. Bull. Int. Ed. 55 (2006) 1768.
[7] S.P. Ghordape, V.S. Darshane, S.G. Dixit, Appl. Catal. A: Gen. 166 (1998) 135.
[8] N. Ma, Y. Yue, W. Hua, Z. Gao, Appl. Catal. A: Gen. 251 (2003) 39.
[9] M.V. Tsodikov, V.Ya. Kugel, E.V. Slivinskii, G.N. Bondarenko, Yu.V. Maksimov, M.A. Alvarez, M.C. Hidalgo, J.A. Navio, Appl. Catal. A: Gen. 193 (2000) 237.
[10] Yu.V. Maksimov, V.V. Matveev, I.P. Suzdalev, M.V. Tsodikov, O.G. Ellert, Hyperfine Interact. 56 (1990) 1983.
[11] B.V. Kuznetsov, S.N. Lanin, T.A. Rakhmanova, V.V. Smirnov, M.V. Tsodikov, D.V. Tarasova, Zh. Fiz. Khim. 81 (2007) 781.
[12] A. Davidov, Molecular Spectroscopy of Oxide Catalyst Surfaces, Wiley, 2003.
[13] N. Sheppard, T.T. Nguyen, in: R.J.H. Clark, R. Hester (Eds.), Advances in Infrared and Raman Spectroscopy, vol. 5, Heyden, London, 1978, p. 67.
[14] K.J. Hadjiivanov, G.N. Vayssilov, Adv. Catal. 47 (2002) 307.
[15] M.A. Haney, J.L. Franklin, J. Phys. Chem. 73 (1969) 4328.
[16] A.S. Medin, V.Yu. Borovkov, V.B. Kazansky, A.G. Pelmentschikov, G.M. Zhidomirov, Zeolites 10 (1990) 668.
[17] C.L. Angell, M.V. Howell, J. Phys. Chem. 73 (1969) 2551.
[18] K.F. Purcell, R.S. Grado, J. Am. Chem. Soc. 88 (1966) 919.
[19] A.V. Kiselev, V.I. Lygin, Infrared Spectra of Surface Compounds, Nauka/Wiley, Moscow/New York, 1975.